International Journal of Progressive Sciences and Technologies (IJPSAT)
ISSN: 2509-0119.

http://ijpsat.ijsht-journals.org
Vol. 26 No. 1 April 2021, pp. 526-541

Structural Characterization of Isolated Siloxaalkane Molecular Gyroscopes via DFTB-based Quantum Mechanical Model

Anant Babu Marahatta[1, 2,*] and Hirohiko Kono[3]

[1]Department of Chemistry, Amrit Science Campus, Tribhuvan University, Kathmandu, Nepal
[2]Department of Civil Engineering, Chemistry Subject Committee, Kathford International College of Engineering and Management (Affiliated to Tribhuvan University), Kathmandu, Nepal
[3]Department of Chemistry, Graduate School of Science, Tohoku University, Sendai, Japan

Abstract – Despite many more improvements in the mathematical formalisms of the DFT model, it is still unable to compute ground state electronic structure of the crystalline macrocyclic molecular compounds (CMMCs) with closed topology at low computational cost. In the recent years, a less computationally complex and relatively fast plus efficient self-consistent-charge density functional based tight binding (SCC-DFTB) scheme has been heavily extended to CMMCs under both periodic and isolated molecular conditions mainly for computing as reliable molecular structures as standard time-dependent DFT. In this study, the SCC-DFTB method is employed to characterize the molecular structures of three different molecular gyroscopes (MGs) encapsulating dihalogen substituted (e.g. ROT-2F and ROT-2Cl) and non-substituted (e.g. ROT-2H) phenylene segments under isolated condition. We realized the SCC-DFTB method a cheap yet decent quantum mechanical model in reproducing one or more X-ray observed equilibrium structures of all these three MGs as well as in deriving as consistently good structural information as DFT method. While elucidating experimentally observed structural deformation mainly in the ROT-2F and ROT-2Cl, the SCC-DFTB computed free-volume units present around their central phenylene segments are also found to be in quantitatively good agreement with those derived by the X-ray and DFT. The results presented here enlighten us about the SCC-DFTB method for adopting it directly in crystalline condition to predict crystal structures and rotational dynamics of these MGs. This theoretical insight will promote SCC-DFTB studies on gyroscopic nanostructures and giant molecular assemblies that attract increasing attention for molecular machinery world.

Keywords – SCC-DFTB, Molecular Gyroscopes, Halogen Substituted Phenylene Rotators, Restricted and Unrestricted Rotation.

I. INTRODUCTION

A density-functional theory (hereafter, DFT) in principle is an exact computational quantum mechanical modelling method for investigating ground state electronic structures of the multi-electron and/or many-body systems (atoms, molecules, and condensed phases) [1-4]. However, the approximate variants of it that are currently being implemented are far from fail-safe. One of its very fundamental problem that has become widely apparent is the lack of proper mathematical formulations to account the substantial effect of long-range attractions or van der Waals (hereafter, vdW) type intra-/inter- molecular interactions existing predominantly in both isolated caged molecular compounds and their giant molecular assemblies [5-10]. Beside this, its inability to derive ground state electronic structures of such type macrocyclic compounds at a low computational cost is another complication. It means, in terms of computational time and complexity as well, the DFT may not be an appropriate and efficient theoretical model to perform quantum mechanical energy minimization calculations while applying either to the isolated or to the crystalline macrocyclic compounds having bridged delocalized π-electron systems (**chart 1**) where vdW force competes significantly with other interactions. So, on one hand the remarkable effect of intra- /inter- molecular vdW interactions has

Corresponding Author: Anant Babu Marahatta

to be addressed quantum mechanically by some computational means; but on the other hand, the computational processes should be cheap yet reasonable while attempting real ground state electronic energy and the global minimum electronic structure theoretically. The extended density functional tight binding (hereafter, DFTB) DFTB+ scheme [11-15] is one of such means whose fundamental formulation is actually based on the DFT but is designed differently mainly for executing Slater-Kirkwood model [16] and Slater-Koster files [17] with a focus on giant molecular assemblies bound each other by dispersion type forces. Unlike DFT model, this theoretical scheme allows us to perform calculations for large and complex molecular systems over long timescales at an extremely low computational cost, but derives the results typical of standard time-dependent DFT. In terms of how DFT Kohn-Sham energy is expanded with respect to charge density fluctuations, DFTB has two different approaches: (a) Non-self-consistent-charge DFTB (NCC-DFTB); the zeroth-order expansion [12-14], and (b) Self-consistent-charge DFTB (hereafter, SCC-DFTB); the second-order expansion [18,19]. Technically, both of them can implement Slater-Kirkwood model and Slater-Koster files (SK-files) computationally and execute the effect of the vdW interactions in stabilizing complex molecular structures significantly [20-22]. But, in terms of computing Mulliken charge distribution in a molecule, the SCC-DFTB is regarded as a more promising theoretical approach as it takes into account charge interactions between the atoms through iterative self-consistent manner [18, 19]. This is why, it is more popularly known among the researchers as a practically suitable quantum mechanical DFTB approach more especially for computing low energy electronic structures of the heteroatomic complex molecular systems like the one shown in **chart 1** [21].

Chart 1[#]

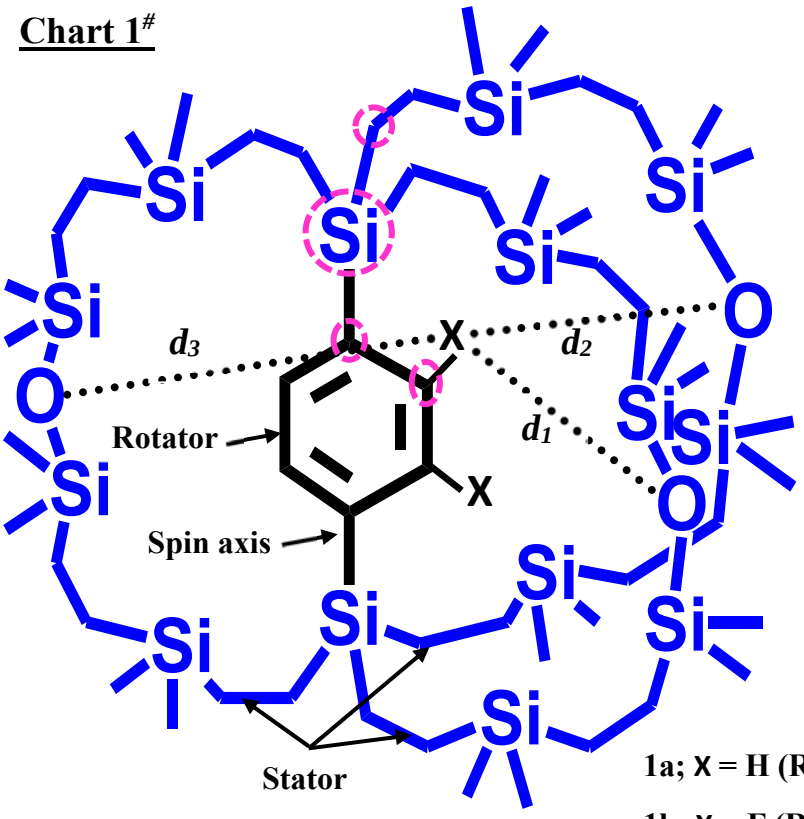

1a; X = H (ROT-2H)

1b; X = F (ROT-2F)

1c; X = Cl (ROT-

[#] It is a model of the siloxaalkane molecular gyroscope reproduced from reference [23]. Two methyl (CH_3) groups attached to each Si atom of each siloxaalkane arm are omitted for clarity. The atoms encircled by pink colored circle form the dihedral angle (ϕ) of the central phenylene rotator. The $d_{OX} = \{d_1, d_2, d_3\}$ estimates the free-volume unit.

In the field of nanotechnology and molecular machinery world, the crystalline macrocyclic compounds with encased phenylene rings of the type displayed in **chart 1** are regarded as the most promising nanomaterials carrying tremendous potentialities in respect to creating varieties of smart, intelligent, and responsive materials due to their amphidynamic behavior: the central phenylene unit (*i.e.* rotator) of each molecule in the crystal undergoes internal rotation with respect to stationary spokes (*i.e.* stator) at temperatures ranging from high to moderate [23-25]. Beside this, such type of uniquely designed and strategically synthesized crystalline compounds with a closed topology and a sufficient free space (free-volume unit) around the rotators are expected to functionalize as nanoscale devices due to their structural flexibility, functionality, and reliability though the related fundamental mechanisms are not fully understood yet. One of the most encouraging examples is to reorient centrally encased dipolar rotators by conserving their internal volume through external stimuli such as electric field, magnetic field, light etc. so that one may realize controllable molecular motions practically [26-28]. Structure wise, each and every molecule in the crystal lattice resembles well to the macroscopic gyroscope used in internal navigation system, and hence, very often called it as a molecular gyroscope [23, 29]. Setaka *et al.* reported experimentally synthesized three different crystalline molecular gyroscopes (**chart 1)** with a nonpolar phenylene rotator (hereafter, ROT-2H, **1a**), and the dipolar halogen substituted rotators: difluorophenylene (hereafter, ROT-2F, **1b**) and dichlorophenylene (hereafter, ROT-2Cl, **1c**) encased into the three siloxaalkane arms elsewhere [23, 24]. Through X-ray crystallography, they confirmed that the rotators of the molecular gyroscopes **1a**, **1b**, and **1c** undergo smooth, restricted, and prevented type rotation between three (position **A**, **B**, and **C**), two (position **A** and **B**), and one stable positions respectively, and the shape of the surrounding siloxaalkane spokes of the **1b**, and **1c** goes through significant deformation while inserting dichloro and difluro units on the central phenylene unit of their precursor module **1a**. The detailed X-ray observations including rotary motions and the experimental synthetic procedures are reported elsewhere [23, 24]. In the same context, present author has already reported theoretical (DFT and DFTB (NCC & SCC)) insights into the molecular structures under isolated and crystalline conditions and real time rotational dynamics of the molecular gyroscope **1a**, and the DFT analysis on the molecular structures of **1b** and **1c** under isolated condition elsewhere [20, 21, 30]. However, the SCC-DFTB studies carried out on **1b** and **1c** have not been reported so far as it computes as accurate low energy ground state electronic structures as DFT at extremely low computational cost and complexity. Therefore, in the present contribution, the X-ray observed molecular structures of both **1b** and **1c** are interpreted under isolated molecular condition by employing SCC-DFTB method, and the experimentally observed structural consequences including the effect of their deformed siloxaalkane spokes to confine their dipolar rotators at the specific positions are examined and quantified theoretically. For the X-ray observed structural validations and the in-depth structural comparisons, the SCC-DFTB produced ground state electronic structure of their precursor molecular analogue **1a** (most stable position is **B**) is used here as a reference. The structure of this paper is organized as: the theoretical approaches and computational methods are outlined in section 2, the results and discussions are presented in section 3, and the conclusions are given in section 4.

II. Computational Details

As the trial structures for geometry optimization of the isolated molecular gyroscopes **1a**, **1b**, and **1c**, the initial coordinates of the atoms were taken directly from the X-ray crystallographic data. For **1a**, the isolated molecule was extracted from the Cartesian coordinates of the unit cell geometry at 223 K (monoclinic crystal) and for **1b** and **1c**, the same was extracted from the unit cell geometry at 273 K (orthorhombic crystal). Since

the dihalogen substituted molecular gyroscopes **1b** and **1c** are molecular analogues of the **1a**, the latter one is taken here as a reference molecule. This is why, only the most stable equilibrium structure (position **B**: dihedral angle = 0.55π) of the **1a** out of its three stable forms (X-ray observed) was optimized under non-crystalline condition by using SCC-DFTB method, whereas for the molecular gyroscope **1b**, both of its degenerate equilibrium **s**tructures that are dissimilar to each other by 1π phenylene flipping were optimized: they are represented hereafter by structure **A** (dihedral angle = 0.56π) and structure **B** (dihedral angle = 1.57π). Unlike **1a** and **1b**, a single fixed structure of the molecular gyroscope **1c** due to having an immobile central unit (dichlorophenylene ring) was also optimized by the same theoretical method. All the experimentally and theoretically derived electronic structures were visualized by *Jmol*: an open-source Java viewer for chemical structures in 3D [31].

While writing the DFTB+ optimizer code, we set series of the DFTB keywords on the basis of users' manual available elsewhere [32]. Accordingly, the Hamiltonian and non-crystalline computations were implemented *via* the keywords "Hamiltonian = DFTB" and "Periodic = No". The specific trial structure was specified explicitly in XYZ format through the general format (keyword: "GenFormat") method. The "conjugate gradient algorithm" was selected as a driver to change the geometry of the input structure, and the force component for controlling the optimization process was set to an *ab initio* level *i.e.*"ForceComponent = 1*e*–6" as its maximal absolute value. No any geometry constraints were specified *i.e.* all the atoms were allowed to move freely while the optimization calculations were on the fly. Moreover, the DFTB keyword "AppendGeometries = Yes" was set to receive the geometry file (in the XYZ-format) containing all the geometries obtained during optimizations. Under "ConvergentForcesOnly" option, the terminology "SCC = YES" was set in order to drive the DFTB+ script to run SCC type calculations so that the geometry optimization can be controlled whether it stops prematurely whenever the SCC cycle does not converge at any geometric step. Similarly, the values for the keywords "SCCTolerance" and "MAXSCCIterations" were fixed to 1*e*−5 and 200 respectively. Additionally, a Slater-Kirkwood type dispersion model [16, 32] was implemented for incorporating the vdW type interactions exist in between the rotators and stators of all the three isolated molecular gyroscopes. For it, the dispersion energy parameter sets available elsewhere [32, 33, 34] and the Slater−Koster files [17, 32] of mio-1-1 set were explicitly used for every pairwise permutation atomic types.

III. Results and Discussions

In general, the SCC type computational procedure involves a self-consistent calculation of the Mulliken charges and a derivation of corresponding nuclear forces [32]. This feature actually makes the SCC-DFTB method highly applicable more especially to heteroatomic complex molecular systems where charge balance between the atoms is crucial. In this study, we optimized the X-ray nuclear coordinates of each molecular gyroscope **1a**, 1b, and **1c** under non-crystalline condition (isolated molecule) using SCC-DFTB method and interpreted theoretically produced equilibrium structures in reference to their X-ray observed molecular geometries. At the beginning, the most stable X-ray produced equilibrium structure (Figure 1(a)) of the molecular gyroscope **1a** was optimized fully without periodic boundary condition (hereafter, PBC), and then two different degenerate X-ray structures **A** and **B** of the **1b** (Figure 2(a) and Figure 3(a)) followed by an X-ray produced single stable form of the **1c** (Figure 4(a)).

Table 1. Experimental vs. Theoretical structural parameters for the central phenylene units of the molecular gyroscopes **1a**, **1b**, and **1c**. The $d_{OX} = \{d_1, d_2, d_3\}$ and rotator dihedral angle ϕ of each molecular gyroscope are defined in **chart 1**. The DFT datasets presented here are reproduced from the previous publication [30] of the same author for comparative purpose.

Molecular Gyroscopes	Bonds	Bond length (nm)			"Free volume" (d_{OX}) $d_{OX} = \{d_1, d_2, d_3\}$ (nm)			Rotator dihedral angle ϕ (π)		
		Expt	DFT	DFTB	Expt	DFT	DFTB	Expt	DFT	DFTB
1a (ROT-2F) Structure **A**	C−F	0.15	0.14	0.138						
	C−C	0.14	0.14	0.136						
	C−H	0.09	0.11	0.110	0.51	0.48	0.481	0.56	0.63	0.63
	C−Si_1	0.19	0.19	0.189	0.84	0.85	0.848			
	C−Si_2	0.19	0.19	0.189	0.95	0.92	0.923			
Structure **B**	C−F	0.15	0.14	0.138						
	C−C	0.14	0.14	0.136			0.511	1.57		
	C−H	0.09	0.11	0.110	0.52	0.51	0.858		1.64	1.64
	C−Si_1	0.19	0.19	0.188	0.84	0.86	0.921			
	C−Si_2	0.19	0.19	0.188	0.94	0.92				
1b (ROT-2Cl)	C−Cl	0.17	0.14	0.148						
	C−C	0.14	0.14	0.139						
	C−H	0.09	0.11	0.101	0.81	0.83	0.828	0.32	0.30	0.30
	C−Si_1	0.19	0.19	0.188	0.84	0.83	0.828			
	C−Si_2	0.19	0.19	0.188	0.87	0.79	0.788			
1c (ROT-2H) (reference molecule)	C−C	0.14	0.14	0.142						
	C−H	0.09	0.11	0.110	0.39	0.41	0.412	0.55	0.31	0.31
	C−Si_1	0.19	0.19	0.191	0.43	0.41	0.411			
	C−Si_2	0.19	0.19	0.191	0.51	0.52	0.518			

These SCC-DFTB converged ground state electronic structures are displayed in Figure 1(b), Figure 2(b), Figure 3(b), and Figure 4(b) respectively. In theoretical chemistry/physics, it is a usual trend of specifying these low energy ground state molecular geometries by determining their specific type bond lengths, bond angles, and dihedral angles because accurate identification of the position of the atomic nuclei in the theoretically converged structures always generates as reliable as experimentally observed structural information. Therefore, the quite essential sets of these structural parameters that are found to be involved directly in describing 3D molecular geometries of all the three molecular gyroscopes **1a**, **1b**, and **1c** more precisely are carefully selected here. The SCC-DFTB computed values of them for the central phenylene (unsubstituted and substituted) units and the siloxaalkane arms of **1a**, **1b**, and **1c** are tabulated along with the corresponding experimental (X-ray determined) and DFT derived values in Table 1 and Table 2 respectively.

As we can see in the second and third column of the Table 1, all the C−C bond lengths of the non-substituted and dihalogen (X = F and Cl) substituted phenylene units of the **1a**, **1b**, and **1c** respectively are found to be in intermediate range while comparing them with the length of a standard C=C double bond (bond length = 0.135 nm) and a C−C single bond (bond length = 0.147 nm). It suggests us that all the three central phenylene units have partial double bond characters responsible for creating some degree of electronic delocalization. Similarly, while monitoring interior and exterior bond angles, and the dihedral angles of these central units (in the X-ray, DFT, and SCC-DFTB derived structures), they are found to be distorted from the respective parameters for the original planar shape of the benzene molecule (all these angular values are excluded in Table 1 as they are considered to be less significant here). Each of these structural distortions is due to the effect of nonbonding type intramolecular interactions taking place between surrounding siloxaalkane arms and central phenylene unit of each molecular gyroscope **1a**, **1b**, and **1c**. In stereochemistry, this interaction is most commonly called steric effects that often arises in each molecular gyroscope from the repulsive forces between the overlapping electron clouds of the central phenylene unit and the surrounding siloxaalkane spokes, and the resulting steric type hindrance is not only responsible to influence the internal shape of the central phenylene unit of each molecular gyroscope but also to impose each unit to adjust in particular position of the free space present inside the static siloxaalkane spokes. Moreover, as listed in the fifth column of Table 1, the phenylene dihedral angle ϕ (it gives us an exact position of the phenylene unit present inside the siloxaalkane spokes and is formed by the four atoms encircled in **chart 1**) for the experimentally produced most stable structure of **1a** is 0.55π (modulo π), the difluorophenylene dihedral angle for the two X-ray degenerate equilibrium structures of **1b** are 0.56π and 1.57π (1π flip), of which structures or dihedral angles are denoted by **A** and **B** respectively, and the dichlorophenylene dihedral angle of the single equilibrium structure of **1c** is 0.32π. By the SCC-DFTB method, these angles are converged to 0.32π (DFT: 0.31π), 0.63π↔1.64π (DFT: 0.63π↔1.64π) (1π flip), and 0.30π (DFT: 0.30π) respectively. As reported experimentally, these theoretically derived data sets confirm that the two stable structures **A** and **B** of **1b** (Figure 2 and Figure 3) are related to each other by 1π flipping of the central difluorophenylene unit. Nevertheless, all these SCC-DFTB derived dihedral angles are found to be resembled well with the hybrid functional DFT derived values mentioned above in the closing parenthesis. Additionally, in terms of reproducing DFT predicted values of the phenylene structural data sets for each molecular gyroscope (Table 1) as well, performance of the SCC-DFTB method is also quite impressive.

According to X-ray analysis, a notable structural deformation in the siloxaalkane arms is observed while substituting two hydrogen atoms of the central phenylene of **1a** by two fluorine (as

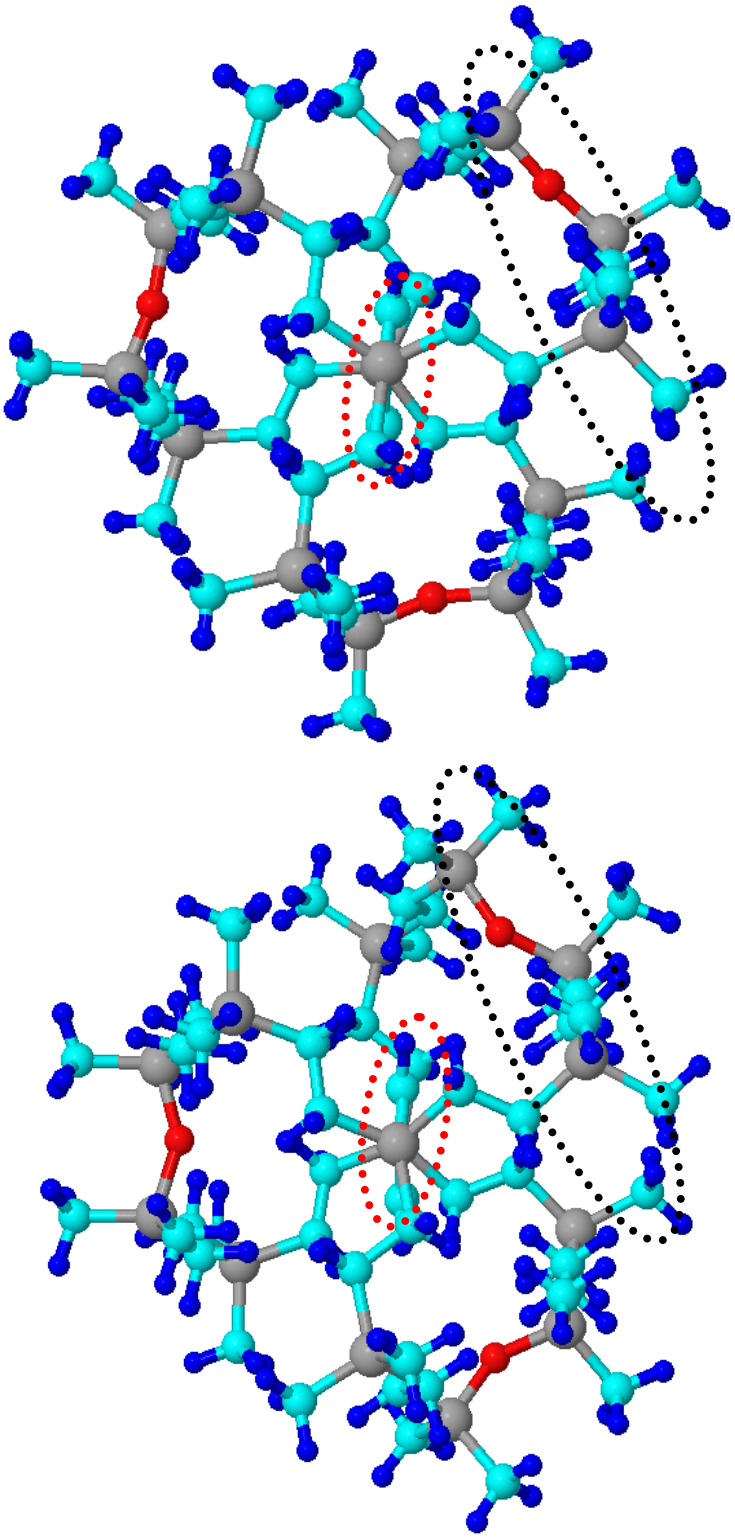

Figure 1. (a) X-ray (b) SCC-DFTB optimized geometry of an isolated ROT-2H molecular gyroscope **1a** viewed along the spin axis. The cyan, blue, dark gray, and red spheroids represent Carbon, Hydrogen, Silicon, and Oxygen atoms respectively. The phenylene rotators and siloxaalkane arms are enclosed by red and black circles respectively.

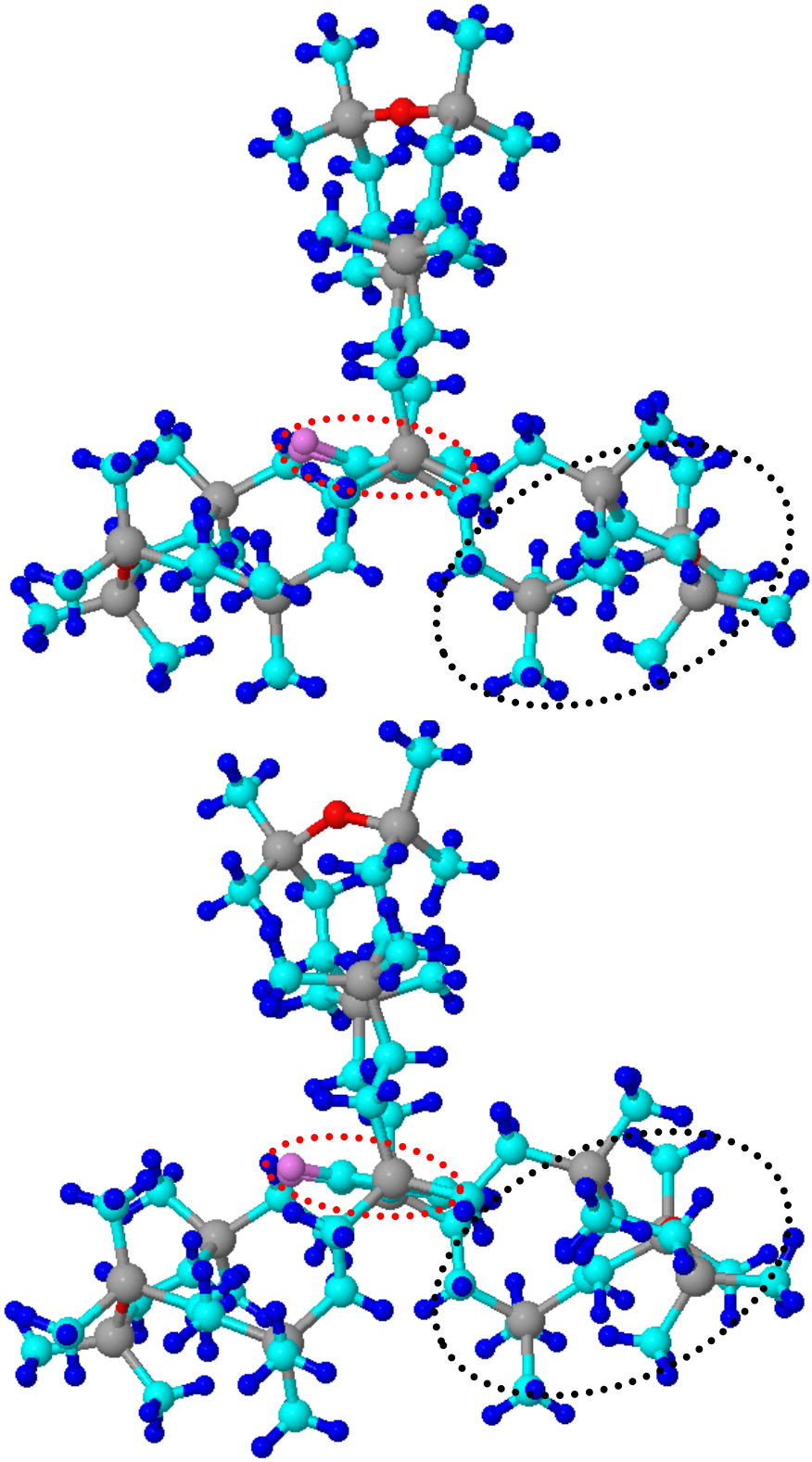

Figure 2. (a) X-ray (b) SCC-DFTB optimized geometry of an isolated ROT-2F molecular gyroscope **1b** (structure **A**) viewed along the spin axis. The cyan, blue, dark gray, red, and violet spheroids represent Carbon, Hydrogen, Silicon, Oxygen, and Fluorine atoms respectively. The difluorophenylene rotators and siloxaalkane arms are enclosed by red and black circles respectively.

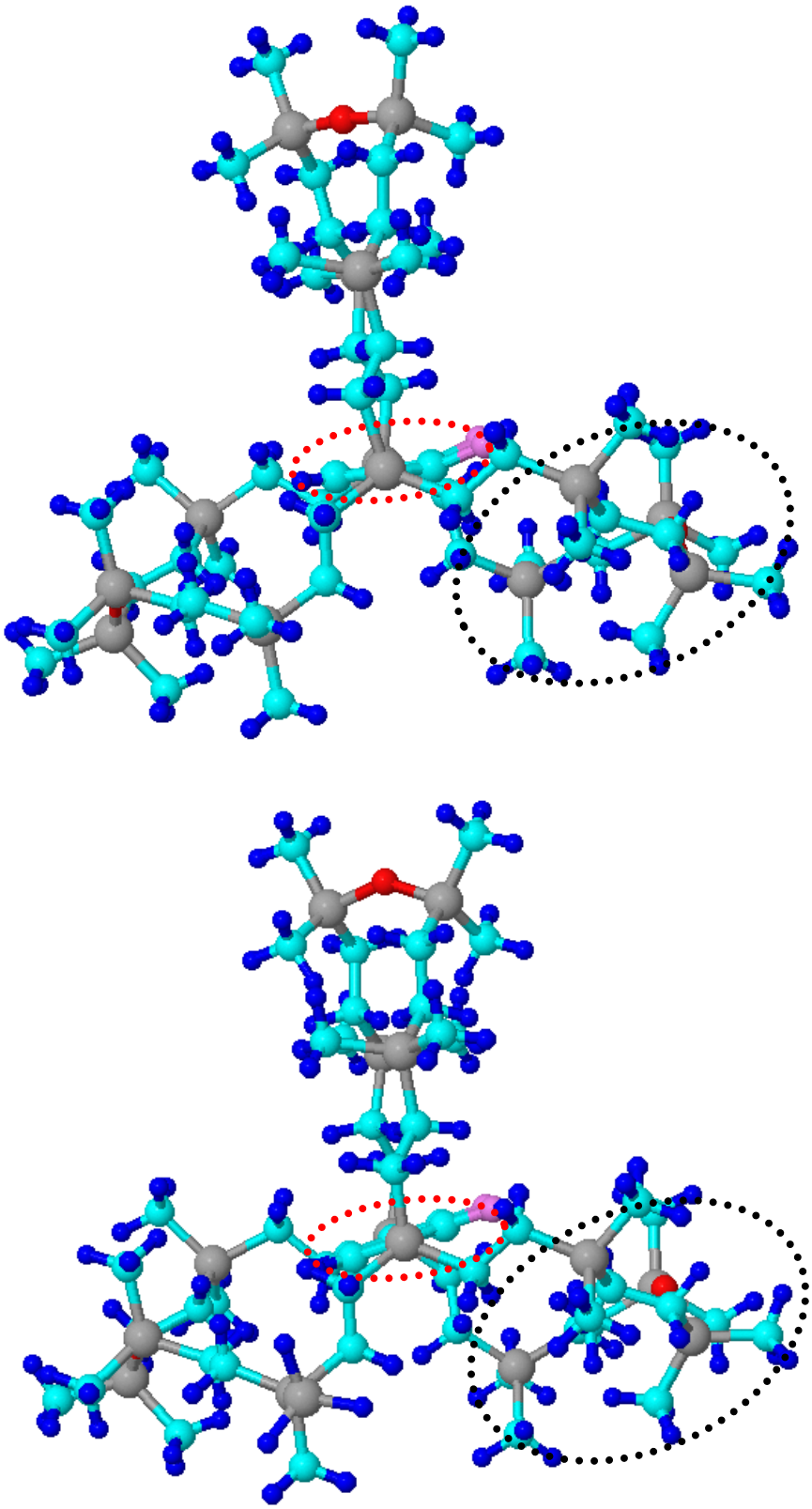

Figure 3. (a) X-ray (b) SCC-DFTB optimized geometry of an isolated ROT-2F molecular gyroscope **1b** (structure **B**) viewed along the spin axis. The cyan, blue, dark gray, red, and violet spheroids represent Carbon, Hydrogen, Silicon, Oxygen, and Fluorine atoms respectively. The difluorophenylene rotators and siloxaalkane arms are enclosed by red and black circles respectively.

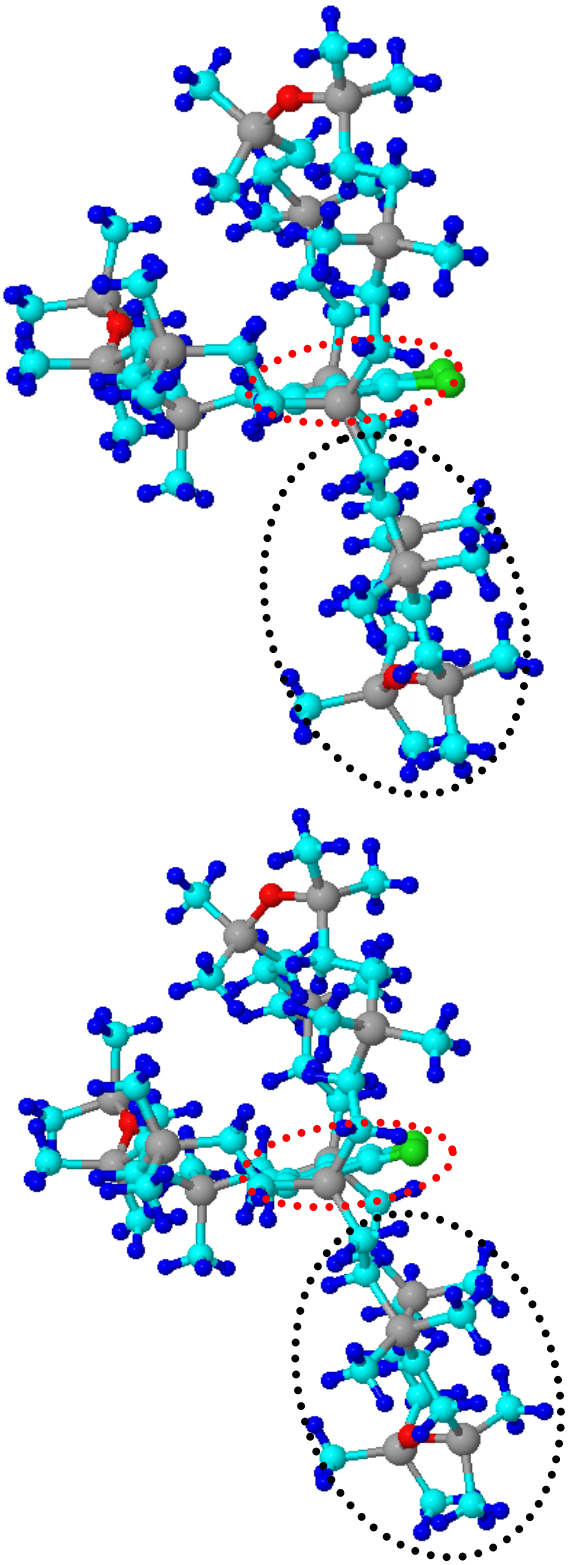

Figure 4. (a) X-ray (b) SCC-DFTB optimized geometry of an isolated ROT-2Cl molecular gyroscope **1c** viewed along the spin axis. The cyan, blue, dark gray, red, and green spheroids represent Carbon, Hydrogen, Silicon, Oxygen, and Chlorine atoms respectively. The dichlorophenylene rotators and siloxaalkane arms are enclosed by red and black circles respectively.

in **1b**) and two chlorine (as in **1c**) atoms [24]. And, these deformed siloxaalkane arms are reported as responsible parts to narrow down the free-volume unit (the volume where the rotator is enclosed by the static framework inside which it moves more or less freely) present around each rotating segment of **1b** and **1c**. But, such a significant structural changes occurred in their static frameworks and their direct impact in phenylene (rotator) movement has not been interpreted quantitatively. Apart from this, the decisive role of them in demonstrating smooth and restricted rotation as observed in **1a** and **1b** respectively or completely prevented rotation as in **1c** has not been clarified well. In general, the intensity of the intra-molecular type interactions (rotator-stator interactions) increases after inserting two halogen atoms in the central phenylene rotator of **1a**, the free-volume unit is also subjected to change side by side (due to a flexible and elastic nature of the siloxaalkane spokes). As a result, the energy barrier faced by each halogen substituted rotator increases which in turn is accountable for its rotational speed at specific temperature. In short, the free-volume unit, rotational energy barrier, and the types of rotation (smooth, restricted, and prevented as in **1a**, **1b**, and **1c** respectively) observed in all three molecular gyroscopes are correlated to each other. This is the reason why free-volume unit present around the rotator of each molecular gyroscope is determined here precisely. Practically, it can be estimated by measuring an intervening space exists in between O atom of each siloxaalkane arm and the nearest X (H in **1a**; F in **1b**; and Cl in **1c**) atom of the central phenylene ring each of which is assigned as d_{OX} = {d_1, d_2, d_3} in **chart 1**. The separate sets of the d_{OX} = {d_1, d_2, d_3} values measured in the theoretically converged (DFT and SCC-DFTB) equilibrium structures of the **1a**, **1b**, and **1c** are listed in the fourth column of Table 1, where they are found to be in close agreement with the respective values measured in the X-ray produced structures. It ascertains that the theoretically produced electronic structure of each molecular gyroscope possess as sufficient free-volume unit as in X-ray produced molecular geometry, implying that no significant changes will occur in the experimentally observed rotational behaviors and dynamics of the central (unsubstituted and substituted) phenylene units while applying SCC-DFTB method under periodic boundary condition.

Accordingly, the experimentally observed notable structural deformation in the siloxaalkane spokes of **1b** and **1c** (in compare to **1a**) can also be described with the help of their d_{OX} = {d_1, d_2, d_3} values. As can be seen in Table 1, the trend of the d_{OX} data sets for three different molecular gyroscopes is found to be in the order **1a < 1b < 1c**. It means all of them need different amount of free-volume units inside their siloxaalkane spokes, *i.e.* **1c** requires the largest free-volume unit as it has to accommodate bulkiest dichlorophenylene unit (atomic size of Cl: 0.99Å), and then to **1b** for hosting second most bulkiest difluorophenylene unit (atomic size of F: 0.64Å) centrally than to **1a** for housing unsubstituted pheylene rotator (atomic size of H: 0.37Å). Thus, it can be concluded that bulkier the central phenylene unit is stronger would be the structural deformation *i.e.* the most bulky dichlorophenylene of **1c** and the second most bulky difluorophenylene of **1b** impel their siloxaalkane spokes quite apart from the center, resulting an outward expansion (molecular balloon) of the latter or distortion of the whole gyroscopic structures from the original framework of their precursor module (reference molecule) **1a**. In terms of creating steric effects to the surrounding siloxaalkane spokes as well, the halogenated phenylene units are more powerful than the non-substituted phenylene unit. This nonbonding effect also makes the siloxaalkane arms puffing out as they have to avoid this effect to achieve gyroscopic structure having sufficient free-volume unit. In a similar way, the smooth, hindered, and prevented type phenylene rotation observed in **1a**, **1b**, and **1c** can also be explained qualitatively as they are directly related to the energy barriers faced by the rotators themselves. Since the bulkiest dichlorophenylene unit of **1c** and

the second most bulkiest difluorophenylene unit of **1b** interacts most and second most strongly with the siloxaalkane arms (intramolecular interactions) than does by the non-substituted phenylene unit of **1a**, the energy barriers experienced by themselves would be in the order: **1a < 1b < 1c**, which means the phenylene unit of **1a** may undergo smooth and facile rotation (low rotational barrier), the difluorophenylene unit of **1b** experiences restricted type flipping motion (comparatively high rotational barrier), and the dichlorophenylene unit of **1c** remains immovable (fixed at a single position) as observed experimentally. Beside this, the prevented type rotation of the dichlorophenylene unit of **1c** is unfavorable structurally as well due to its size, and inappropriate and unfriendly orientation of the two Cl atoms towards their three siloxaalkane arms as can be seen in Figure 4. All these noteworthy explanations directly make us to adopt SCC-DFTB method in studying **1b** and **1c** type crystalline gyroscopic molecular assemblies in future more particularly for investigating their molecular structures and the rotary dynamics under PBC as we applied earlier to their molecular analogue **1a** and reported the results elsewhere [20, 21].

Again, due to the flexible and elastic properties of the three chemically identical siloxaalkane arms of each molecular gyroscope **1a**, **1b**, and **1c**, and their inward and outward dilation while accommodating variably sized rotating units, examining change in bond lengths and angles of their specific bonds further gives us an indirect way to quantify the free-volume units. The theoretically (DFT and SCC-DFTB) and X-ray determined average bond lengths and angles are listed in the third column of Table 2. The careful analyses of them confirm that there is no any significant changes in the bond lengths associated with C atom of the siloxaalkane arms (C−C, C−H, and C−Si) take place while replacing phenylene rotator of **1a** by the difluorophenylene or dichlorophenylene. In contrary, the three sets of Si−O−Si bond angles and an average Si−O bond length in three siloxaalkane arms of each molecular gyroscope are found to vary significantly. This is because the bulkier difluorophenylene and dichlorophenylene units repel their siloxaalkane arms strongly and force them to expand outward (increase in free-volume), resulting a variation in the bond lengths and angles. More importantly, while comparing experimental and theoretical Si−O−Si bond angles and Si−O bond lengths quantitatively, the significant discrepancies are observed. However, this is in good agreement if we consider the partial ionic and double bond characters of the Si−O−Si linkages which not only govern their strength but also contribute to exceptional conformational flexibility of the $-(Si-O)_x-$ chains and their segments [35].

Table 2. Experimental vs. Theoretical structural parameters for each siloxaalkane arm of the molecular gyroscopes **1a**, **1b**, and **1c**. The DFT datasets presented here are reproduced from the previous publication [30] of the same author for comparative purpose.

Molecular gyroscopes	Si-O-Si angle (θ) (π)			Bonds	Bond lengths (nm)		
	X-ray	DFT	DFTB		X-ray	DFT	DFTB
1b (ROT-2F)				C−C	0.15	0.15	0.152
Structure **A**	0.97	0.78	0.78	C−H	0.10	0.11	0.109
	0.84	0.75	0.75	C−Si	0.19	0.19	0.191

Structure **B**	0.84	0.74	0.74	Si−O	0.16	0.17	0.172
				C−C	0.15	0.15	0.152
	0.97	0.78	0.78	C−H	0.10	0.11	0.110
	0.84	0.75	0.75	C−Si	0.19	0.19	0.191
	0.84	0.74	0.74	Si−O	0.16	0.18	0.179
				C−C	0.15	0.15	0.151
1c (ROT-2Cl)	0.79	0.74	0.74	C−H	0.10	0.11	0.110
	0.80	0.76	0.76	C−Si	0.19	0.19	0.189
	0.83	0.79	0.79	Si−O	0.16	0.18	0.181
				C−C	0.15	0.15	0.151
1a (ROT-2H) (reference molecule)	0.91	0.78	0.78	C−H	0.10	0.11	0.110
	0.94	0.78	0.78	C−Si	0.18	0.18	0.179
	0.96	0.82	0.82	Si−O	0.16	0.17	0.171

Altogether, if we compare the X-ray and SCC-DFTB optimized structures of each isolated siloxaalkane molecular gyroscope **1a**, **1b**, and **1c** displayed in Figure 1 to Figure 4, we reconfirm the above mentioned features for the optimized structures that the orientation of the central phenylene units and the conformations of the surrounding siloxaalkane spokes are well reproduced. Beside this, the orientation and conformation of the methyl groups attached to each siloxaalkane arm are also not noticeably different. Though the DFT derived electronic structures of **1a**, **1b**, and **1c** and their structural information are not shown here in detailed, we found that they agree semi-quantitatively with the corresponding SCC-DFTB produced structures and related structural parameters. This actually supports the DFTB+ scheme, a comparatively more computationally cheap and efficient model, applicable to gyroscopic nanostructures and molecular machinery world.

IV. Conclusion

In this theoretical insight, the ground state electronic structures of the experimentally synthesized three different siloxaalkane molecular gyroscopes having central polar and nonpolar phenylene units: ROT-2F (difluorophenylene), ROT-2Cl (dichlorophenylene) and ROT-2H (phenylene) are investigated theoretically under non-crystalline condition by employing computationally cheap yet decent SCC approach of the DFTB method. Along with this, comparatively more convincing theoretical ways for describing X-ray observed smooth, restricted, and prevented type phenylene rotation in ROT-2H, ROT-2F, and ROT-2Cl respectively are also presented. Basically, the ROT-2H is considered here as a reference molecule for the sake of examining

experimentally observed significant structural deformation in the ROT-2F and ROT-2Cl that arises after substituting two hydrogen atoms of the ROT-2H's central phenylene by two fluorine and two chlorine atoms. The unanimous choice of this reference molecule here is due to being a molecular analogue and precursor module for the ROT-2F and ROT-2Cl molecular gyroscopes synthetically.

In order to verify X-ray produced stable structures theoretically, we first optimized the most stable X-ray structure of the ROT-2H (out of its three stable forms) followed by two degenerate X-ray structures (structure **A** and **B**) of the ROT-2F and a single stable form of the ROT-2Cl separately without endorsing PBC criteria, and compared all these theoretically produced molecular structures with the corresponding X-ray structures on the basis of practically measured structural data sets: bond lengths, bond angles, and dihedral angles. We found no significant structural deviation among the SCC-DFTB and X-ray derived equilibrium structures except in the $-(Si-O)_x-$ chains and Si−O−Si linkages of each siloxaalkane arm of each molecular gyroscope. But, the inconsistencies we noted in their structural information are in a satisfactory range if we recognize their partial ionic and double bond characters. Moreover, we determined the free-volume units present around the central phenylene segment of each SCC-DFTB produced structure of the molecular gyroscope and elucidated an experimentally observed structural deformation in the siloxaalkane spokes of ROT-2F and ROT-2Cl quantitatively. We concluded that the notable structural deformation in them is mostly occurred as a result of avoiding steric hindrance of their central difluorophenylene and dichlorophenylene segments by surrounding siloxaalkane spokes, and the same effect is responsible to change their free-volume units which in turn decides smooth, restricted, or prevented type phenylene rotation as observed experimentally in ROT-2H, ROT-2F, and ROT-2Cl molecular gyroscopes respectively.

ACKNOWLEDGEMENT

The authors would like to express sincere thanks to Prof. W. Setaka, Tokushima Bunri University, Japan for providing unit cell X-ray geometry of each siloxaalkane molecular gyroscope: ROT-2H, ROT-2F, and ROT-2Cl. Part of this work was carried out through the high-performance computing systems available at Cyberscience Center-Tohoku University, Sendai, Japan.

REFERENCES

[1] W. Kohn, L. J. Sham, "Self-consistent equations including exchange and correlation effects", *Physical Review*, Vol. **140**, No. **4A**, pp. **A1133**–**A1138**, **1965**.

[2] A. B. Marahatta, "A DFT Analysis for the Electronic Structure, Mulliken Charges Distribution and Frontier Molecular Orbitals of Monolayer Graphene Sheet", *International Journal of Progressive Sciences and Technologies*, Vol. **16**, No. **1**, pp. **51**–**65**, **2019**.

[3] P. Hohenberg, W. Kohn, "Inhomogeneous Electron Gas", *Physical Review B*, Vol. **136**, No. **3B**, pp. **864**–**871**, **1964**.

[4] A. B. Marahatta, "DFT Study on Ground State Electronic Structures of Simple to Complex Molecular Specimens", *International Journal of Progressive Sciences and Technologies*, Vol. **19**, No. **1**, pp. **100**–**112**, **2020**.

[5] A. J. Cohen, P. M. Sánchez, W. Yang, "Insights into current limitations of density functional theory" *Science*, Vol. **321**, Issue **5890**, pp. **792**–**794**, **2008**.

[6] D. Buckingham, P. W. Fowler, J. M. Hudson, "Theoretical studies of van der Waals molecules and intermolecular forces", *Chemical Reviews*, Vol. **88**, No. **6**, pp. **963–988**, **1988**.

[7] J. Tao, J. P. Perdew, A. Ruzsinszky, "Accurate van der Waals coefficients from density functional theory", *Proceedings of the National Academy of Sciences of the U. S. A*., Vol **109,** Issue **1**, pp. **18–21**, **2012**.

[8] A. D. Becke, "Density-functional thermochemistry. III. The role of exact exchange", *Journal of Chemical Physics*, Vol. **98**, Issue **7**, pp. **5648–5652**, **1993**.

[9] J. P. Perdew, K. Burke, M. Ernzerhof, "Generalized Gradient Approximation Made Simple", *Physical Review Letter*, Vol. **77**, pp. **3865–3868**, **1996**.

[10] J. Tao, J. P. Perdew, V. N. Staroverov, G. E. Scuseria, " Climbing the density functional ladder: nonempirical meta-generalized gradient approximation designed for molecules and solids", *Physical Review Letter*, Vol. **91**, Issue **14**, 146401-1**–146401-4**, **2003**.

[11] G. Seifert, "Tight-Binding Density Functional Theory: An Approximate Kohn−Sham DFT Scheme", *Journal of Physical Chemistry A*, Vol. **111**, Issue **26**, pp. **5609–5613**, **2007**.

[12] G. Zheng, S. Irle, K. Morokuma, "Performance of the DFTB method in comparison to DFT and semiempirical methods for geometries and energies of C_{20}–C_{86} fullerene isomers", *Chemical Physics Letter*, Vol. **412**, Issue **1–3**, pp. **210–216**, **2005**.

[13] B. Aradi, B. Hourahine, Th. Frauenheim, "DFTB+, a Sparse Matrix-Based Implementation of the DFTB Method", *Journal of Physical Chemistry A*, Vol. **111**, Issue **26**, pp. **5678–5684**, **2007**.

[14] M. Elstner, D. Porezag, G. Jungnickel, J. Elsner, M. Haugk, Th. Frauenheim, S. Suhai, G. Seifert, " Self-consistent-charge density-functional tight-binding method for simulations of complex materials properties", *Physical Review B*, Vol. **58**, pp. **7260–7268**, **1998**.

[15] T. Frauenheim, G. Seifert, M. Elstner, T. Niehaus, C. Köhler, M. Amkreutz, M. Sternberg, Z. Hajnal, A. D.Carlo, S. Suhai, " Atomistic simulations of complex materials: ground-state and excited-state properties", *Journal of Physics: Condensed Matter*, Vol. **14**, pp. **3015–3047**, **2002**.

[16] Koehler, Z. Hajnal, P. Deak, Th. Frauenheim, S. Suhai, "Theoretical investigation of carbon defects and diffusion in α-quartz", *Physical Review B*, Vol. **64**, pp. **085333**, **2001**.

[17] M. Elstner, Th. Frauenheim, E. Kaxiras, G. Seifert, S. Suhai, "A Self-Consistent Charge Density-Functional Based Tight-Binding Scheme for Large Biomolecules", *Physical Status Solidi B,* Vol. **217**, Issue **1**, pp. **357–376**, **2000**.

[18] M. Elstner, P. Hobza, Th. Frauenheim, S. Suhai, E. Kaxiras, " Hydrogen bonding and stacking interactions of nucleic acid base pairs: A density-functional-theory based treatment", *Journal of Chemical Physics*, Vol. **114**, Issue **12**, pp. **5149–5155**, **2001**.

[19] E. Rauls, R. Gutierrez, J. Elsner, Th. Frauenheim, "Stoichiometric and non-stoichiometric (1010) and (1120) surfaces in 2H–SiC: a theoretical study", *Solid State Communications*, Vol. **111**, Issue **8**, pp. **459–464**, **1999**.

[20] A. B. Marahatta, M. Kanno, K. Hoki, W. Setaka, S. Irle, H. Kono, "Theoretical Investigation of the Structures and Dynamics of Crystalline Molecular Gyroscopes", *Journal of Physical Chemistry C*, Vol. **116**, pp. **24845–24854**, **2012**.

[21] A. B. Marahatta, H. Kono, "Performance of NCC- and SCC-DFTB Methods for Geometries and Energies of Crystalline Molecular Gyroscope", *International Journal of Innovative Research and Advanced Studies*, Vol. **6**, Issue **5**, pp. **180–185**, **2019**.

[22] A. B. Marahatta, "Geometry Optimization Skills of DFTB: Simple to Complex Molecular Systems", *International Journal of Progressive Sciences and Technologies*, Vol. **15**, No. **2**, pp. **263–277**, **2019**.

[23] W. Setaka, S. Ohmizu, C. Kabuto, M. Kira, "A Molecular Gyroscope Having Phenylene Rotator Encased in Three-Spoke Silicon-Based Stator", *Chemistry Letter*, Vol. **36**, pp. **1076–1077**, **2007**.

[24] W. Setaka, S. Ohmizu, M. Kira, "Molecular gyroscope having a halogen-substituted *p*-phenylene rotator and silaalkane chain stators", *Chemistry Letter*, Vol. **39**, pp. **468–469**, **2010**.

[25] W. Setaka, K. Yamaguchi, "Thermal modulation of birefringence observed in a crystalline molecular gyrotop", *Proceedings of the National Academy of Sciences of the U. S. A*., Vol. **109**, pp. **9271–9275**, **2012**.

[26] V. Balzani, M. Venturi, A. Credi, "*Molecular Devices and machines: A Journey into the Nano World*", Wiley-VCH: Weinheim, **2003**.

[27] T. R. Kelley, "Molecular Machines. Topics in Current Chemistry", Springer publication, **2005**.

[28] Z. Dominguez, H. Dang, M. J. Strouse, M. A. Garcia-Garibay, "Molecular compasses and gyroscopes. III. Dynamics of a phenylene rotor and clathrated benzene in a slipping-gear crystal lattice", *Journal of American Chemical Society*, Vol. **124**, Issue **26**, pp. **7719–7727**, **2002**.

[29] R. D. Horansky, L. I. Clarke, J. C. Price, T. V. Khuong, P. D. Jarowski, M. A. Garcia-Garibay, "Dielectric response of a dipolar molecular rotor crystal", *Physical Review B*, Vol. **72**, pp. **014302-1–014302-5**, **2005**.

[30] A. B. Marahatta, H. Kono, "Comparative Theoretical Study on the Electronic Structures of the Isolated Molecular Gyroscopes with Polar and Nonpolar Phenylene Rotator", *International Journal of Progressive Sciences and Technologies*, Vol. **20**, No. **1**, pp. **109–122**, **2020**.

[31] Jmol: an open-source Java viewer for chemical structures in 3D. *http://www.jmol.org/*

[32] DFTB+ manual. *https://dftbplus.org/fileadmin/DFTBPLUS/public/dftbplus/latest/manual. pdf*

[33] Y. K. Kang and M. S. Jhon, "Additivity of atomic static polarizabilities and dispersion coefficients", *Theoretica Chimica Acta*, Vol. **61**, pp. **41–48**, **1982**.

[34] K. J. Miller, "Additivity methods in molecular polarizability", *Journal of American Chemical Society*, Vol. **112**, pp. **8533–8542**, **1990**.

[35] G. J. Richard, C. Julian, "Silicon-Containing Polymers: The Science and Technology of Their Synthesis and Applications", Springer publication, **2000**.